Electrochemical CO$_2$ Reduction – A Critical View on Fundamentals, Materials and Applications

Julien Durst*[a], Alexander Rudnev*[bc], Abhijit Dutta[b], Yongchun Fu[b], Juan Herranz[a], Veerabhadrarao Kaliginedi[b], Akiyoshi Kuzume[b], Anastasia A. Permyakova[a], Yohan Paratcha[a], Peter Broekmann[b], and Thomas J. Schmidt[ad]

Abstract: The electrochemical reduction of CO$_2$ has been extensively studied over the past decades. Nevertheless, this topic has been tackled so far only by using a very fundamental approach and mostly by trying to improve kinetics and selectivities toward specific products in half-cell configurations and liquid-based electrolytes. The main drawback of this approach is that, due to the low solubility of CO$_2$ in water, the maximum CO$_2$ reduction current which could be drawn falls in the range of 0.01–0.02 A cm^{-2}. This is at least an order of magnitude lower current density than the requirement to make CO$_2$-electrolysis a technically and economically feasible option for transformation of CO$_2$ into chemical feedstock or fuel thereby closing the CO$_2$ cycle. This work attempts to give a short overview on the status of electrochemical CO$_2$ reduction with respect to challenges at the electrolysis cell as well as at the catalyst level. We will critically discuss possible pathways to increase both operating current density and conversion efficiency in order to close the gap with established energy conversion technologies.

Keywords: CO$_2$ reduction reaction · Electrolyzer · Energy conversion · Gas diffusion electrode · Power-to-gas/liquid

1. Introduction

Reducing the emissions of greenhouse gases by increasing the fraction of renewable energies at the expense of fossil fuels is one of the most important scientific, technological and economic challenges humankind is currently facing.[1] To achieve this aim and to tackle the undesired effects of climate change, considerable efforts are being undertaken worldwide to develop effective CO$_2$ capture and storage technologies.[2–4] Based on these, one can think how to re-cycle CO$_2$ to more valuable products. Its electrochemical conversion into carbon-neutral products might be considered as one promising approach towards reducing atmospheric CO$_2$ and storing a surplus of renewable energies at the same time. In

principle, the electrochemical CO$_2$ reduction reaction (CO$_2$RR) could be performed in an electrolysis type of device, called a *CO$_2$-electrolyzer* or *co-electrolyzer*. This energy conversion device can be considered as the central part of *power-to-gas/power-to-liquid* processes that operate using the excess of electricity generated from renewable sources.[5,6] In analogy with a water electrolyzer, a CO$_2$-electrolysis cell is fed with H$_2$O at the anode, where the oxygen evolution reaction (OER) occurs, whereas CO$_2$ is supplied to the cathode where it is electrochemically reduced. The *electric* energy would be *chemically* stored either in the form of feedstock chemicals (starting material for further synthesis) or as fuels. Ideally, CO$_2$RR should yield to a single energy-rich compound. However, selective CO$_2$ conversion into specific reaction products remains a challenging task at present due to the multiple proton-coupled electron transfer steps involved in this reaction.[7]

This work attempts to give a short overview on the status of electrochemical CO$_2$ reduction with respect to challenges at the catalysts as well as at the electrolysis cell level. It critically discusses possible pathways to increase both operating current density and conversion efficiency in order to make co-electrolysis a technically and economically feasible option for the transformation of CO$_2$ into a chemical feedstock or fuel thereby closing the CO$_2$ cycle.

2. Identifying Valuable CO$_2$RR Products

Table 1 provides a simple cost analysis for all major CO$_2$ reaction products that can be obtained from a CO$_2$-electrolysis cell. For designing and establishing an economically reasonable CO$_2$ conversion process one needs first to estimate the total costs for the electrochemical production of specific CO$_2$RR products and to compare these in a second step with data from well-established chemical synthesis routes. As a benchmark for our approach, we use data for H$_2$ production from alkaline water electrolysis, an already established and commercially available energy storage technology. In the case of alkaline water electrolysis, large-scale energy storage plants can daily produce ~1000 kg$_{H2}$ with an electric energy at $0.05 kWh^{-1}. Under these conditions, the price for H$_2$ production reaches ~ $4 kg$_{H2}$$^{-1}$ (Table 1). Main contributions to the total production costs originate from electricity (58%) and capital expenses (32%).[8,9] The most severe drawback of the alkaline water electrolysis technology is its low operating current density of ~0.2 A cm^{-2}. Nevertheless, when compared to proton exchange membrane (PEM) electrolyzers, which are operated at current densities that are up to one order of magnitude higher than those of the alkaline electrolyzers, there is no major benefit using PEM-based electrolyzers. The reasons

Correspondence: Dr. J. Durst[a], Dr. A. Rudnev[b]
E-mail: julien.durst@psi.ch; rudnev@dcb.unibe.ch
[a]Electrochemistry Laboratory
Paul Scherrer Institut (PSI)
CH-5232 Villigen, Switzerland
[b]Department of Chemistry and Biochemistry
University of Bern
Freiestrasse 3, CH-3012 Bern, Switzerland
[c]A.N. Frumkin Institute of Physical Chemistry and Electrochemistry
Russian Academy of Sciences
Leninskii pr. 31, Moscow 119991, Russia
[d]Laboratory of Physical Chemistry
ETH Zürich, 8093 Zürich, Switzerland
*These authors contributed equally to this work

are related to higher component costs in case of the PEM electrolyzers. In addition, the PEM electrolyzers typically target only small forecourt applications (daily production of *ca.* ~10–100 kg_{H_2}).[10,11]

Based on these numbers, it is possible to estimate the production costs for specific CO_2RR products under the assumption that the capital costs are similar for both alkaline water and CO_2 electrolyzers. In a first step, we calculate the production volumes per electrolysis unit by assuming similar operating current densities (~0.2 A cm^{-2}) as applied in alkaline water electrolyzers. Eqn. (1) is used to convert the production volume of H_2 (V_{H_2} in kg_{H_2} h^{-1}) into the respective production volumes of specific CO_2RR products (V_{CxHyOz} in kg h^{-1}) *via* the ratio of the molar masses (M in g mol^{-1}) and the number of electrons exchanged to produce 1 mol of product (n_{e^-}, 2 for H_2/CO/$HCOO^-$, 6 for CH_3OH, 8 for CH_4, 12 for C_2H_4).

$$V_{CxHyOz} = V_{H2} \cdot \frac{M_{CxHyOz}}{M_{H_2}} \cdot \frac{n_{e^-,H_2}}{n_{e^-,CxHyOz}} \quad [1]$$

Production volumes per electrolysis unit are listed in Table 1 for various CO_2RR products. Further assuming that a CO_2 electrolysis cell operates at a similar energy efficiency as an alkaline water electrolyzer, the production costs of 1 mol CO_2RR product become a fixed number, namely $8 \cdot 10^{-3}$ $mol_{product}^{-1}$, no matter which specific product is considered. The production cost of a specific CO_2RR product per unit of mass can then be calculated by multiplying $8 \cdot 10^{-3}$ $mol_{product}^{-1}$ with the molar mass of the respective CO_2RR product. As can be seen in Table 1, due to its low molecular weight, hydrogen is the most expensive electrolysis product when normalized to its mass. Before commenting on the CO_2RR product costs, it has to be stressed that CO_2RR kinetics are significantly slower compared to the hydrogen evolution reaction (HER) kinetics thus resulting in much higher CO_2RR overpotentials that need to be applied to the cathode. This actually leads to a lower energy efficiency of the CO_2R-electrolysis, roughly half of that of an alkaline water electrolyzer (for a more detailed discussion we refer to the next section). As a consequence, the CO_2RR product costs will rise accordingly (let us assume by a factor of 2) due to the increased energy consumption during operation. More realistic production costs for CH_4, C_2H_4, CO, $HCOO^-$ and CH_3OH are therefore expected to be $4, $3.2, $0.48, $0.34 and $1.4 kg^{-1}, respectively. From an analysis of Table 1 it becomes obvious that the CO_2-electrolysis will not be competitive for all of the possible reaction products. In particular the production costs for CH_4 and C_2H_4 ($4 and $3.2 kg^{-1}, respectively) will be far higher compared to more conventional production routes ($0.08 and $1.4 kg^{-1}, respectively). This price difference becomes even larger for methane when considering its extraction from natural gas. The conversion of CO_2 into CH_4 and C_2H_4 by electrolysis appears therefore to be highly counterproductive, at least from an economic point of view. The same is true for methanol, which can be considered as an energy carrier such as H_2.[12] What seems to be much more promising is the generation of CO from CO_2. CO production costs ranging from $0.27 to $0.54 kg^{-1} are well below the current market price of $0.65 kg^{-1} (Table 1). In addition, the global market for CO is extremely large as reflected by the annual CO production of 210,000 Mt. CO in combination with H_2 (syngas) serves as an important chemical precursor for a number of industrial processes (*e.g.* Fischer-Tropsch synthesis). Another interesting product of the CO_2RR is formate (it should be kept in mind that only formic acid, obtained by the protonation of formate, is a valuable product). Estimated productions costs are factors of 2–4 lower than the current market price for formate/formic acid ($0.34 vs. $0.8–1.2 kg^{-1}, Table 1). Formic acid is widely used as a preservative and an antibacterial agent in livestock feed. The market for formic acid with a yearly production of 0.8 Mt is, however, much smaller compared to the global demand for CO/syngas. An electrochemical conversion of CO_2 into formate/formic acid has a high potential to become an economically competitive process.

3. Energy Efficiency of CO_2 Electrolysis

The cost analysis presented above relies on the basic assumption that CO_2–electrolysis cells would reach similar current densities to those featured in alkaline water electrolyzers (0.2 A cm_{geo}^{-2}).[25] However, such large current densities cannot be reached by CO_2 electrolyzers based on liquid aqueous reaction environments. This general limitation originates from the low solubility of CO_2 in aqueous electrolyte solutions (~30 mM in H_2O at atmospheric pressure) thus resulting in diffusion-limited current densities which typically do not exceed values of 0.03 A cm_{geo}^{-2}. These are one order of magnitude below the current densities reported for alkaline water elec-

Table 1. Current and estimated costs of production by CO_2-electrolysis for H_2, CH_4, C_2H_4, $HCOO^-$ and CH_3OH.

Product	Produced by	Current market price [$ kg^{-1}]	Current production volume [Mt y^{-1}]	Production price by electrolysis[a] [$ kg^{-1}]	Production volume per electrolysis unit[b] [Mt y^{-1}]
H_2	steam reforming, partial oxidation of methane or gasification of coal[13]	2-4[14]	65	4	0.0003
CH_4	methanogenesis or hydrogenation of CO_2[15]	<0.08[15]	2400[16]	2-4	0.0007
C_2H_4	pyrolysis or vapocracking[17]	0.8-1.5[18]	141[17]	1.6–3.2	0.0009
CO	Boudouard reaction[19]	0.65	210000	0.27–0.54	0.005
$HCOO^-$/HCOOH	hydrolysis from methyl formate and formamide[20] or by-product of acetic acid production	0.8-1.2[20]	0.8[21]	0.17–0.34	0.008
CH_3OH	From natural gas, coal, biomass, waste[22,23]	0.4-0.6[23,24]	100[23]	0.70–1.4	0.002

[a]The lowest price is calculated by assuming the cell device efficiency of an alkaline water electrolyzer. The highest price is obtained by considering that a co-electrolysis device is operating at half the efficiency of an alkaline water electrolyzer and so that the production price of individual products will be twice higher.
[b]Estimated on the basis of a daily production from an alkaline water electrolyzer of ca. 1000 kg_{H_2}

trolyzers. From a technical point of view, there could be in addition a severe contamination issue associated with aqueous reaction environments. A ppm level of metallic contaminations, typically present in aqueous electrolyte solutions, would already be sufficient to irreversibly poison the catalyst surface during CO_2 electrolysis, *e.g.* with Fe trace contaminants that get electroplated during operation.[26] These metallic contaminations further shift the selectivity of the electrode reaction towards hydrogen formation thus lowering the faradaic efficiency (FE), ratio of CO_2RR current to total current, for specific products of the CO_2RR. These circumstances require a careful and most likely rather costly purification of the electrolyte solutions for the CO_2RR. Contributions to the production costs originating from these extra electrolyte purification steps are not considered in Table 1.

Under the assumption of only kinetic and ohmic losses, the cell potential E_{cell} for the CO_2 electrolysis can be derived on the basis of Eqn. (2):

$$E_{cell} = E_{rev} + \eta_{anode} + \eta_{cathode} + i \cdot R_{ohmic} \quad [2]$$

E_{rev} corresponds to the reversible potential (listed in Table 3 further down). The $i \cdot R_{ohmic}$ term in Eqn. (2) accounts for voltage losses caused by the finite ionic conductivity of the electrolyte solution (see Table 4 for typical R_{ohmic} values). The η_{anode} and $\eta_{cathode}$ terms in Eqn. (2) refer to the overpotentials of the anodic (OER) and cathodic (CO_2RR) half-cell reactions, respectively. Reliable information on the CO_2RR and OER reaction kinetics specifically for gas diffusion configurations are, however, rare in literature.[27–29] For the sake of simplicity we therefore estimate CO_2RR and OER overpotentials from experimental data available for polycrystalline catalyst materials in aqueous reaction environments. For such considerations we assume that the particular catalyst performance does not alter when going from an ideal aqueous environment to a gas diffusion configuration.[30–36] Catalyst materials that perform best toward specific CO_2RR product are listed in Table 2. Their kinetic performance can be derived from Fig. 1A which relates current density and applied overpotential in a semi-logarithmic plot (η_{kin} vs $\log(i_{kin})$). The linear correlations observed between η_{kin} and $\log(i_{kin})$ in Fig. 1A are clear fingerprints of Tafel behaviors in this specific current density range (with 100–150 mV decade^{-1} Tafel slopes), which confirm that these curves are dominantly charge-transfer controlled and not limited by mass transport. On the basis of this catalytic performance for model electrodes having roughness factors of *ca.* 1 cm_{metal}^2 cm_{geo}^{-2}, we compute kinetically controlled curves (not shown) for technical electrodes prepared from metal nanoparticles with different diameters and corresponding surface areas,[37–39] again listed in Table 2. For doing this, we assume that the kinetic performance of the catalysts will not be affected by the transition between aqueous and gas-phase reaction media (as it has been demonstrated for fuel cells[40]) nor by particle-size effects.

Based on the CO_2RR and OER kinetic overpotentials (Fig. 1A) and the electrolyte resistances (Table 4), the cell voltage E_{cell} is calculated from Eqn. (2) as function of the applied current and is shown for the various electrolysis cells in Fig. 1B. From these theoretical polarization curves, device efficiencies ($\xi_{Electrolyzer}$) are estimated using Eqn. (3):

$$\xi_{Electrolyzer} = \frac{\Delta H^0}{\Delta G^0} \cdot \frac{E_{rev}}{E_{cell}} \quad [3]$$

ΔH^0 and ΔG^0 in Eqn. (3) relate to enthalpies and respective Gibbs free energies of the overall (co-)electrolyzer cell reactions as listed in Table 3. The validity of our approach can be verified on the basis of the calculated efficiency for a PEM electrolyzer, in good agreement with performance data reported elsewhere.[41] It can be seen in Fig. 1A that CO and $HCOO^-$ are the
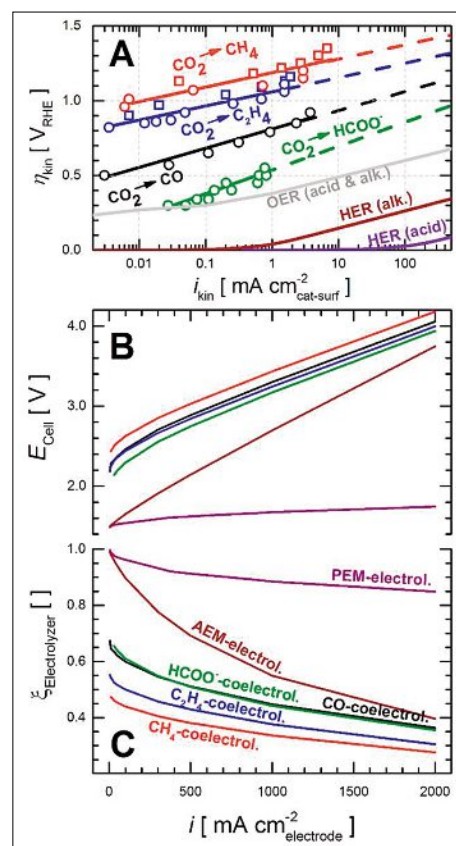

Fig. 1. Tafel plots and computed (co-)electrolyzer polarization curves and efficiencies. (A) Relation between partial CO_2-reduction currents and overpotentials in 0.1–0.5 M $KHCO_3$ for the reduction of CO_2 on Cu, Ag or Sn, to yield C_2H_4 and CH_4,[31] CO[34] or formate,[32] respectively. The OER curve is estimated on the basis of the data for the Ir-surface,[30] whereby similar activities are observed in acid and alkaline electrolyte. The HER curves are computed using the Butler-Volmer equation and a transfer coefficient of 0.5 and considering the exchange current density values at 25 °C reported in refs. [35] and [42] (for alkaline and acid media, respectively). (B) Polarization curves computed on the basis of the kinetic data in (A), calculating the geometric currents on the basis of the roughness factors listed in Table 2 and estimating E_{cell} with Eqn. (2) and the R_{ohmic}-values in Table 4. (C) Corresponding (co-)electrolyzer efficiencies, computed by substituting the E_{cell} values in (B) and the thermodynamic data in Table 3 into Eqn. (3).

Table 2. Summary of the half reactions and corresponding catalysts at play in (co-)electrolysis cells, along with the electrode roughness factor values projected on the basis of the catalyst loading and average particle size.

Half Cell Reaction	Catalyst	Loading[a] [$mg_{cat} \cdot cm_{geo}^{-2}$]	d_{part}[b] [nm]	Surface area[c] [$m_{metal}^2 \cdot g_{cat}^{-1}$]	Roughness Factor [$cm_{metal}^2 \cdot cm_{geo}^{-2}$]
$CO_2 + 8H^+ + 8e^- \rightleftharpoons CH_4 + 2H_2O$	Cu	5	50	13	670
$2CO_2 + 12H^+ + 12e^- \rightleftharpoons C_2H_4 + 4H_2O$					
$CO_2 + 2H^+ + 2e^- \rightleftharpoons CO + H_2O$	Ag	5	100	5	270
$CO_2 + H^+ + 2e^- \rightleftharpoons HCOO^-$	Sn	5	100	7	430
$2H^+ + 2e^- \rightleftharpoons H_2$	Pt	0.5	3	90	450
$H_2O \rightleftharpoons \frac{1}{2}O_2 + 2H^+ + 2e^-$	IrO_2	1.5	10	50	750

[a]Typical catalyst loading values in alkaline and PEM-electrolyzers.[43] [b]Average particle size diameters based on values reported in the literature for Cu black particles,[39] carbon-supported Ag-nanoparticles,[37] and battery Sn-anodes.[38] The values for Pt and IrO_2 are typical of fuel cells and electrolyzers.[43] [c]Assuming spherical metal particles with all of their area exposed to the reaction medium.

CO_2RR products generated with the lowest overpotential (–0.6 and –0.45 V at 0.2 A cm_{geo}^{-2}), as opposed to C_2H_4 and CH_4 (–0.9 and –1.1 V at 0.2 A cm_{geo}^{-2}). This is in line with our previous conclusions that CO and $HCCO^-$ are the most economically interesting products to be considered from the CO_2RR (Table 1). Ultimately, when comparing all electrolyzers efficiencies (Fig. 1C), the CO_2 to CO or $HCOO^-$ electrolyzers have efficiencies in the range 55–60% at 0.2 A cm_{geo}^{-2}, close to that of an alkaline water electrolyzer (80%). Moreover, the projected efficiency of the CO_2-electrolysis cells would certainly benefit from improvements in CO_2-reduction electrocatalysis, and from the development of membranes with better ionic conductivities. This optimization is therefore addressed in the following sections.

4. CO_2 Electrolysis Cell Design

Our cost estimation for the diverse CO_2RR products (Table 1) was based on the assumption that the electrolysis device operates at the same current density as an alkaline water electrolyzer (0.2 A cm_{geo}^{-2}). However, as already discussed above, these current densities cannot be achieved by electrolysis cells that use liquid electrolytes as source for dissolved CO_2 reactants. In the following we will review several electrolysis cell designs that would allow achieving high current densities for the CO_2RR. These different types of electrolyzers can be classified according to the nature of the electrolyte used in these devices.

4.1 CO_2 Electrolysis at Low pH Conditions

PEM electrolysis configurations, based on the use of 50–100 µm thick proton exchange membrane acting as electrolyte and separator between the anode and cathode, allow an order of magnitude larger current densities than alkaline water electrolyzers.[41] The pH in the membrane and at the gas diffusion electrode/electrolyte interfaces is highly acidic with pH ≈ 0 where the HER, considered as a parasitic side reaction for the CO_2RR, proceeds at the highest rates compared to other pH conditions.[42] As an example, Delacourt *et al*. used a PEM electrolysis configuration with a silver-based GDE as cathode that was fed with gaseous CO_2 as reactant.[27] In this case no CO_2 reduction product was detected (only H_2) although silver is considered as the most active catalyst material for the CO_2 to CO pathway. Even if most reports claim that the high HER currents are the sole reason why cathode electrodes cannot be polarized below CO_2 reduction onset potential, it should be noted that

Table 3. Full cell reactions and corresponding enthalpy, free energy and reversible potential values (at standard conditions and 25 °C) for the (co-)electrolysis cells considered in this study.

Overall (co-)electrolyzer reaction	$-\Delta H^0$ [kJ mol^{-1}]	$-\Delta G^0$ [kJ mol^{-1}]	E_{rev} [V]
H_2O (l) $\rightleftharpoons H_2 + \frac{1}{2}O_2$	286.0	237.3	1.23
$CO_2 + H_2O$ (l) $\rightleftharpoons HCOOH + \frac{1}{2}O_2$	270.3	285.5	1.48
$CO_2 \rightleftharpoons CO + \frac{1}{2}O_2$	283.1	257.2	1.34
$CO_2 + 2H_2O$ (l) $\rightleftharpoons CH_4 + 2O_2$	890.8	818.4	1.06
$2CO_2 + 2H_2O$ (l) $\rightleftharpoons C_2H_4 + 3O_2$	1411.2	1331.2	1.15

Table 4. Ionic conductivity and corresponding resistivity values for the membrane electrolytes implemented in the (co-)electrolyzers.

| Device	Membrane	Ionic conductivity[a] [mS·cm^{-1}]	R_{ohmic}[b] [Ω·cm$_{geo}^2$]
PEM-electrolyzer	Perfluorosulfonated	100	0.05
Alkaline water electrolyzers	25-35% KOH	–	1[9]
Co-electrolysis cell	Anion-exchange, carbonated	7	0.700

[a]Conductivity values for OH-exchanged and carbonated alkaline membranes extracted from ref. [44]. [b]Estimated on the basis of 50 µm thick membranes.

since PEM electrolyzer configurations allow 3 orders of magnitude higher current than electrochemical measurements in liquid electrolyte to be achieved, and assuming a Tafel slope for the HER of *ca*. 120 mV decade^{-1},[36] an electrode interface in a PEM electrolyzer can be polarized at *ca*. 360 mV lower potential than in a liquid-based electrochemical device. Nonetheless, this extended potential domain probed in the work of Delacourt *et al*. did not allow them to detect any CO_2 reduction product. As a conclusion, it is more than likely that a CO_2-electrolysis configuration adapted from a PEM electrolyzer would not be a suitable solution.

4.2 CO_2 Electrolysis in an AEM-type Configuration (High / Neutral pH Conditions)

The counterpart of the PEM technology in terms of pH conditions is an anion exchange membrane (AEM). Here, OH^- species are exchanged through quaternary ammonium moieties that are covalently attached to the polymer backbone of the membrane. The AEM regulates the pH at the electrode/membrane interface to a value close to 14.[45,46] Moreover, the use of an AEM, in a so-called AEM electrolyzer device, would allow similar current densities to PEM electrolyzers with the advantage of using noble-metal free anode electrodes for the oxygen evolution reaction.[47–49] It is in particular the alkaline pH which makes the AEM configuration attractive for the CO_2 electrolysis since the FEs of the CO_2RR

are reported to be significantly higher at elevated pHs. In this context it is interesting to note that the initially high pH of 14 in a pristine AEM cannot be maintained in presence of CO_2, where the following equilibrium reaction occurs:[50]

$$(OH^-)_{membrane} + CO_2 \rightleftharpoons (HCO_3^-)_{membrane}$$
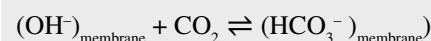
and the pH is expected to regulate in the range of 7–10.

A CO_2 electrolysis test based on an AEM electrolyte has been conducted using a silver-based gas diffusion electrode as cathode material.[27] Here, the HER was still favored over the CO_2RR thus resulting in low FEs in the range of only 1%.[27] Further studies utilizing the most recent and stable versions of AEMs[46] would need to be undertaken in order to rationalize these results and to clarify whether a CO_2-electrolysis configuration adapted from an AEM electrolyzer can be a suitable solution.

4.3 CO_2 Electrolysis at Neutral pH Conditions

Studies performed in liquid electrolyte solutions identified an optimum pH range for the CO_2RR from 7 to 10. It has further been reported that not only the pH but also the nature of anionic and cationic species in the aqueous electrolyte solution has a great influence on the particular mechanism of CO_2 reduction and the resulting FEs (the interested reader is referred to

ref. [7]). Several electrolysis designs have already been reported in literature for such near-neutral pH conditions and these cell configurations can be grouped into two main kinds: either the electrolyte remains stagnant, *e.g.* immobilized by a matrix, or the liquid electrolyte is flushed in a flow-cell type of reactor. A prime example of the first kind of cell design is proposed in the work of Delacourt *et al.* where a Nafion® membrane in a potassium-form was utilized.[27] Some features of this approach resemble the design of a PEM electrolyzer. However, in this present case the carriers for the ion current are the K$^+$ ions that are transported across the polymer membrane. Moreover, the reactants are dissolved in liquid (aqueous) media and transported by convection to the anode (*e.g.* KOH solution for OER) and cathode (CO$_2$ saturated 0.5M KHCO$_3$ for CO$_2$RR), respectively, in order to balance exchanged charges from the cathodic and anodic reactions. From a performance point of view, the small currents (~0.02 A cm$_{geo}^{-2}$) can be attributed to limitations caused by the solubility of CO$_2$ in the KHCO$_3$ solution. Moreover, the FEs (40% of the total currents) are still far below the expected FEs reported for silver catalysts.[27] A similar approach as the one just described would consist of using AEM electrolysis cell configuration with the circulation of a carbonate/bicarbonate solution in the cathode compartment. This approach has been demonstrated to be effective for water electrolysis[51] and could be test-proofed for CO$_2$ electrolysis. Both of these cell configurations are depicted in Fig. 2A. Overall, several drawbacks arise from the use of a neutral immobilized electrolyte configuration. First, the current carrier (K$^+$, HCO$_3^-$) has to be supplied by the catholyte. This implies that the cathode interface would again consist of a CO$_2$-saturated liquid electrolyte, and so that the CO$_2$-electrolysis cell would be limited to small current densities (0.01–0.03 A cm^{-2}) even though this limiting current could be increased by working under higher CO$_2$ pressure conditions.[52] The second drawback is related to the high level of purity required for the catholyte, where traces of metal cations at the ppm level could lead to much higher rates of hydrogen evolved at the expense of CO$_2$ reduced.[26] Finally the durability of this configuration might be an issue since continuous operation will ultimately lead to the build up of a pH gradient between both electrodes.

To overcome some of these technical limitations, Delacourt *et al.* introduced a dual solid electrolyte configuration consisting of an 800 µm thick glass fiber impregnated with 0.5 M KHCO$_3$ and being in contact with the cathode whereas an additional PEM is in contact with the anode. The cathode can be fed with a humidified

stream of CO$_2$ whereas the anode is exposed to a liquid aqueous solution for the OER.[27] With this dual solid electrolyte design CO$_2$RR current densities of up to ~0.140 A cm^{-2} were achieved for the reduction of CO$_2$ to CO on a silver-based GDE.[53] These current densities are at present the highest reported in literature for the CO$_2$RR. However, there are several drawbacks associated with the cell design proposed by Delacourt *et al.* First, by having the anode and cathode operating under different pH conditions, one introduces an additional loss to the cell voltage (0.059 V per pH unit difference between anode and cathode). The second drawback is related to the overall thickness of the buffer layer. Assuming an ionic conductivity of 10 mS cm^{-1}, the ohmic drop across the 800 µm buffer layer would amount to 1.6 V for a current density of 0.200 A cm^{-2}. This tremendous IR drop would be highly disadvantageous in terms of cell performance. The overall cell efficiency could, however, be significantly improved for instance by replacing the 800 µm buffer layer by a 50 µm thick AEM (such as those used for alkaline fuel cell applications[54]). Another alternative to the glass fiber used by Delacourt *et al.* would be a OH$^-$ or HCO$_3^-$-doped polybenzimidazole (PBI) membrane, as depicted in Fig. 2B. This membrane, when doped with H$_3$PO$_4$, is typically used in high temperature fuel cells,[55] and some attempts were already made to incorporate KOH into the membrane for alkaline electrolysis of fuel cell operation.[56,57] Such a modified cell design with a dual electrolyte configuration, also enabling straightforward collection of gaseous and liquid products, is foreseen

as one of the most promising electrolysis configuration.

An alternative approach for an improved cell design enabling higher CO$_2$RR current densities was developed by Kenis and coworkers (for the detailed description of this cell design the interested reader might refer to refs [28,58–60]). This design is based on a combined (liquid) flow cell and gas diffusion type of reactor where a liquid electrolyte is flushed between two fixed GDEs. This concept of a 'floating' GDE is known to enable very fast diffusion rates.[61] Products of the CO$_2$RR (*e.g.* non-volatile formate) are then released into the liquid electrolyte stream on the inner side of the cathode (Fig. 2A). With regard to the CO$_2$RR, high current densities of 0.130 A cm^{-2} for HCOO$^-$ production[28] and 0.06 A cm^{-2} for CO production have been reported for this cell design.[62] These results also prove the versatility of this cell design. Not only (volatile) gaseous reaction products (*e.g.* CO) can be obtained at high current densities but also liquid (non-volatile) products such as formate.

As electrolyte, a highly concentrated aqueous (bi)carbonate could be used. The high solubility of the Cs and Rb salts (up to 25 mol%) can provide a highly concentrated electrolyte with conductivities up to 100 mS cm^{-1} and allow operation at temperatures above 100 °C at atmospheric pressure.[63,64] It should be kept in mind that since liquid electrolytes are involved in this approach, the same concerns regarding the purity of the electrolytes need to be addressed, as discussed above. Alternatively, also non-aqueous electrolyte solutions might be used in this configuration. Their CO$_2$ solubility is higher than in aque-

A)   PBI+KHCO$_3$ or AEM

Cathode: $3CO_2 + H_2O + 2e^- \rightarrow CO + 2HCO_3^-$

CO$_2$ →   HCO$_3^-$ ↓

GDE
AEM or PBI + KHCO$_3$
GDE
Current collector
Flowfields

H$_2$O →

Anode: $4HCO_3^- \rightarrow O_2 + 2H_2O + 4CO_2 + 4e^-$

B)   Nafion//AEM or Nafion//PBI+KHCO$_3$

Cathode: $3CO_2 + H_2O + 2e^- \rightarrow CO + 2HCO_3^-$

CO$_2$ →
H$_2$O ↑   HCO$_3^-$ ↓
H$^+$ ↑

GDE
AEM/ PBI+KHCO$_3$
Nafion ®
GDE

H$_2$O →

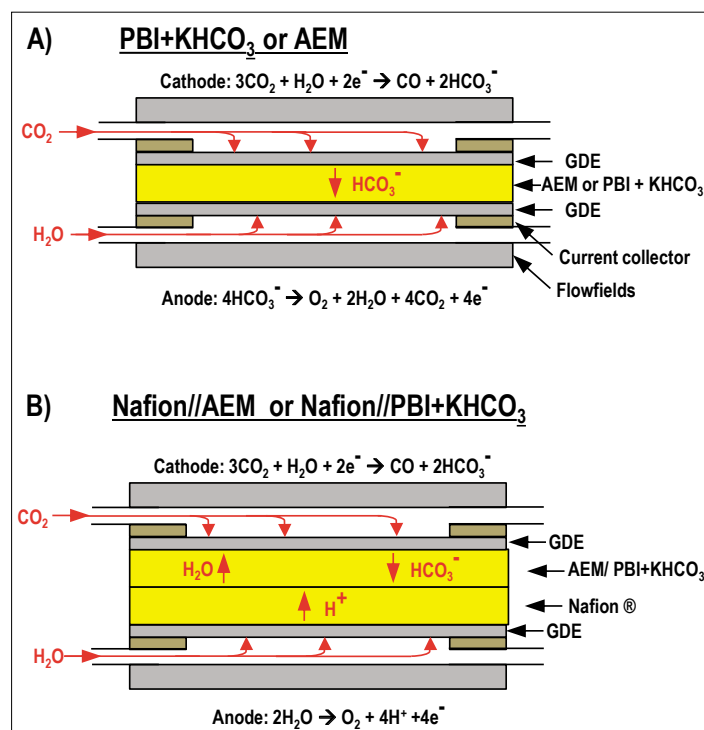Anode: $2H_2O \rightarrow O_2 + 4H^+ + 4e^-$

Fig. 2. Graphical summary of the CO$_2$-electrolysis configurations operating at similar current densities as an alkaline water electrolyzer cell. Note that all the electrochemical reactions are written here to yield CO, but could have been written to yield any kind of other CO$_2$ reduction product.

ous environments (*e.g.* acetonitrile shows a CO_2 solubility which is higher by factor 8 compared to water). The same is valid for room-temperature ionic liquids (RTILs).[65,66] The use of ionic liquids is also attractive due to their ability to capture selectively CO_2 from a diluted gas stream.[66] Their use in such a flow-cell design is, however, restricted to those having a low viscosity. What makes ILs promising electrolytes also for such flow cell devices is their ability to even catalyze the CO_2RR. It was demonstrated that imidazolium-based RTILs dramatically decrease the overpotential for CO_2 reduction particularly in water/RTIL mixtures.[67] Rosen *et al.* used 18 mol% Emim-BF_4 (1-ethyl-3-methylimidazolium tetrafluoroborate) in water as a catholyte in a flow electrochemical reactor. A few recent works have also demonstrated highly selective CO_2RR toward CO on nanostructured metallic catalysts (Ag, Bi) in RTILs and RTIL/acetonitrile.[68–70]

In this part, we have reviewed all the possible CO_2-electrolysis cell configurations, which would allow closing the gap in terms of operating current density with respect to an alkaline water electrolyzer. All these arrangements rely on the use of a GDE for an optimal transport of reactant and reaction products in the gas phase. In order to maximize the number of triple phase boundaries (defined as the presence at the same place of an active catalyst site, CO_2 and electrolyte) and to decrease the kinetic overpotential, the next step should consequently be how to design such GDE with the highest possible roughness factors *i.e.* high $cm^2_{catalyst}$ cm^{-2}_{geo} values. This part will therefore focus on understanding how CO_2 reduction kinetics could be increased, and in the meantime HER currents be suppressed, when engineering electrocatalysts at the micro- and the nano-scale.

5. Electrode Materials for CO_2 Electrolysis

5.1 *Electrodes for Formate Production*

The products and rates of CO_2 electroreduction are affected strongly by the nature and structure of catalytic materials as well as electrolyte solution composition. Numerous half- and full-cell studies were performed to elucidate the key factors influencing CO_2 conversion. As we mentioned above, formic acid and CO would be desirable products in CO_2 electroreduction. The catalytic materials selective for formate production are listed in a recent review article[71] and include: metallic Pb, Hg, In, Sn,[28,72–77] Pd,[78,79] SnO_2,[32,77,80] and metallo-organic complexes.[81] In order to reach sufficient current densities GDEs

are used. Fig. 3 demonstrates the plot of operational potentials and corresponding partial current densities for formate and CO production in CO_2 electroreduction on different GDEs. A few data points are given for non-GDEs.

It is rather difficult to compare the performances of different catalyst materials reported by different research groups, as the CO_2 electrolysis was conducted under different conditions (electrolyte, pH, cell configuration). However, we can distinguish certain trends. The highest current densities for formate production, up to ~0.13 A cm^{-2}, were obtained on unsupported Sn GDEs[28] (solid squares in Fig. 3A). We notice that among s- and p-metals, Sn catalysts seem to be the most promising catalytic material, as it is rather inexpensive, less toxic than *e.g.* lead, and has a very good selectivity for formate. A few recent studies explored SnO_2 as a catalyst for CO_2 electroreduction and reported better kinetics and selectivity toward formate production at such catalysts as compared to Sn.[77,80,82] However, the stability of SnO_2 under operando conditions (rather negative potential of CO_2 reduction), or any oxide phase in general, is still an issue to be addressed. Rather low overpotentials were found for formate production on Pd[79] and Ru-Pd[83] catalysts (star and pentagon in Fig. 3A) with FEs up to 100% operating potentials approximately 0.5 V below the values observed for Sn catalysts. However, the high price of Pd needs to be considered before implementing such a catalyst in CO_2 electrolysis devices.

Review of the literature data showed that the energy efficiency for formate production on different catalysts as obtained in full-cell studies typically has not exceeded 50% even at current densities <0.02 A cm^{-2} and dropped with higher current densities. Such energy efficiency is considerably smaller than the expected maximal efficiency calculated above (Fig. 1C), and is not satisfactory yet.

5.2 *Electrodes for Carbon Monoxide Production*

The reduction of CO_2 to CO (or syngas, CO + H_2) is very attractive, as it can be used as a feedstock for synthetic fuel production *via* Fischer-Tropsch processes. Electrochemical CO formation from CO_2 is favored by Ag, Au and Zn catalysts.[7] Use of water-free electrolyte solutions such as aprotic solvents and ionic liquids also increases the FE for CO production. Fig. 3B displays the relationship between operating potentials and partial current densities for CO formation on different electrodes taken from various full-cell studies. One can see that GDEs with unsupported Ag NPs display relatively good performance reaching partial current densities up to 0.115 A cm^{-2} at E =-0.8 V_{RHE}. A considerably lower performance and FE for CO was found for carbon-supported Ag NPs (40 wt%, dot-centered squares in Fig. 3B):[91] in order to obtain partial current densities of CO production one needed to apply 0.2–0.3 V more negative potential as compared to unsupported Ag NPs (solid squares). However, the use of TiO_2 as a support with 40 wt% loading of Ag (empty squares) allowed reaching similar kinetics of CO_2RR as unsupported Ag NPs (solid squares) but with much lower silver loading. In general, it is better to avoid a carbon support, as it increases the current efficiency of HER. Due to the high surface area of the carbon support, the contribution of HER in overall cathodic process can be very significant.[92] The energy efficiencies for CO production are 40–60% at partial current densities up to 0.115 A cm^{-2}, which is 50% higher than the efficiencies for formate production (Fig. 1B). Normally, the FE of HER increases with increasing the cell voltage. However, since hydrogen gas is a component of syngas, total energy efficiencies for CO + H_2 production are similar to those depicted in Fig. 1C. Importantly, the CO/H_2 ratio can be readily tuned by changing cell voltage[27,29] and potentially by the right choice of the catalyst system.

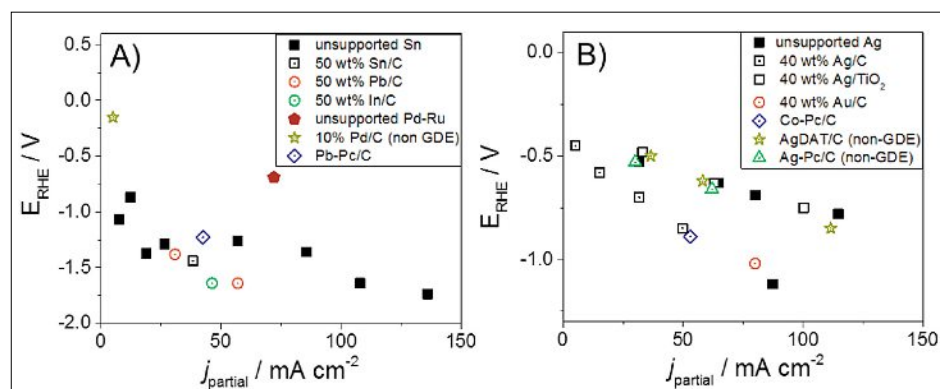

Fig. 3. Potential versus partial current density obtained on GDEs of different compositions for formation of: (A) formate/formic acid[28,72,76,81,83–87] and (B) CO.[53,59,81,88–91] Solid symbols correspond to unsupported metallic catalysts, dot-centered symbols – to carbon supported, empty symbols – to TiO_2-supported. Non-GDEs are indicated in the legend. Details are given in the text.

A recent review postulated the importance of the catalyst morphology for kinetics and even selectivity of CO_2RR.[70] Many examples demonstrated that nanostructured and/or nanosized electrodes could significantly decrease the overpotential of CO_2RR as compared to conventional bulk electrodes. The use of such catalysts also allows high current densities to be reached (respective to geometric area and the mass of catalyst material), which is due to not only a large actual surface area, but also a larger number of active sites for CO_2RR on nanostructured surfaces.[93] The catalytic effect of metallic nanostructured electrodes can be enhanced by introducing additional foreign metals, forming bimetallic nanostructures, such as alloys, core-shell and thin-film configurations[94] (Fig. 4A). The catalytic properties of bimetallic catalysts can be tuned by the choice of foreign metals, chemical composition, morphology of the nanostructures (size, shape and configuration) and capping agents, providing intrinsic functionality different from that of mono-metallic catalysts. Bimetallic catalysts have been studied for many electrochemical reactions, such as oxygen reduction, hydrogen evolution, CO and alcohol oxidation. However, they are scarcely studied on CO_2RR to date.

5.3 Electrodes Modified with Ligands and Complexes

Besides metal surfaces and nanoparticles, nitrogen-rich ligands or metal complexes deposited on the electrode surface also showed promising results for electroreduction CO_2 to formate or CO (Fig. 4B). For example, FEs close to 100% at 70 mA cm^{-2} were achieved on metal-phthalocyanine complexes M-Pc, where M = Co, Ni, Pd, Ag[81,88,89] (dot-centered romb and triangle in Fig. 3B). Promising results were

obtained in a flow cell on carbon-supported, nitrogen-based organometallic Ag catalysts.[89] At the same potential, the current densities of CO formation form CO_2 on e.g. silver 3,5-diamino-1,2,4-triazole supported on carbon (AgDAT/C) were similar to those achieved on Ag-based GDEs (star-symbols in Fig. 3B), but comparatively at much lower silver loading.

Alternatively, nitrogen-rich ligands (for example pyridine, bipyridine, benzimidazole and their polymers) and metal complexes with transition metal centers which are dissolved in an electrolyte solution are also promising (co-)catalysts for electrochemical reduction of CO_2 to CO or formate (Fig. 4C).[95,96] By tuning the structure of the metal complex/ligand, one can tune the stability of the CO_2-adduct which dictates the selectivity of the final product formation. In the past four decades, numerous metal complexes based on the transition metals ruthenium, rhenium, iridium, cobalt, nickel, palladium, silver, copper, iron and manganese (both mono- and dinuclear) were proposed for CO_2 electroreduction, which are based on different families of metal complexes with macrocyclic ligands, with phosphine ligands and with polypyridyl ligands in the electrolyte solution.[95,96] Although some proposed mechanisms suggested such additives acted as homogeneous catalysts for CO_2RR, it seems that in the presence of transition metal complexes or nitrogen-rich ligands the efficiency of CO_2 reduction also depends on the cathode material. As an example, nickel cyclams chemisorbed on mercury were reported to show an enhanced catalytic activity compared an inert electrode such as glassy carbon.[95,97–99] This fact indicates that the ability of an electrode material to adsorb the organic compounds plays an important role in

the CO_2 electrocatalytic reduction in the presence of organic ligands or metal complexes. Based on these results, we believe that the use of metal nanoparticles modified with nitrogen-rich metal complexes or ligands (Fig. 4D) might be a promising approach towards the development of effective catalysts for CO_2RR with a well-controlled catalyst selectivity and stability.

6. Conclusion

The direct electrochemical conversion of CO_2 into more valuable products can be considered as a highly promising approach for the concentration reduction of atmospheric CO_2 and at the same time for the storage of a surplus of renewable energy (e.g. from solar and wind sources) in form of a reduced carbon compound. A careful analysis of the estimated production costs and process efficiencies revealed that CO (or syngas) and formate are the economically most favorable reaction products of such CO_2 conversion. Their electrochemical generation can be considered as potentially competitive with their conventional and well-established routes of production.

In this critical review we, however, identified a number of challenges which still need to be addressed before CO_2 electrolysis can become economically viable. New designs of CO_2 electrolyzers need to be developed which allow for much higher current densities (0.2 A cm$_{geo}^{-2}$) than recently reported for state-of-the-art CO_2 electrolyzer set-ups. In conventional electrolyzers where an aqueous environment serves as CO_2 source it is the CO_2 mass transfer which typically limits the CO_2 conversion rate. An improved CO_2 mass transfer can be achieved by using non-aqueous electrolytes (e.g. ionic liquids) that reveal a much higher CO_2 solubility (>one order of magnitude as compared to aqueous media). An alternative and most likely even more promising approach to tackle CO_2 mass transfer issues is based on a gas-diffusion type of cell design where the cathode is directly fed with the gaseous CO_2 reactant. Concepts of alkaline and acidic water electrolyzers with proton exchange membranes (PEMs) and anion exchange membranes (AEMs) as their key elements can be in part transferred to the design of a more efficient CO_2 electrolyzer. These concepts and in particular the membrane design still need to be adjusted to the specific requirements of the CO_2 electroreduction reaction. The same is valid for the design and chemical composition of the gas diffusion electrodes. In the case of the CO_2 electroreduction there is no need to disperse the electrocatalytically active material on a carbon support since the common catalysts for CO_2 electroreduction are abundant and cheap (e.g. Sn for
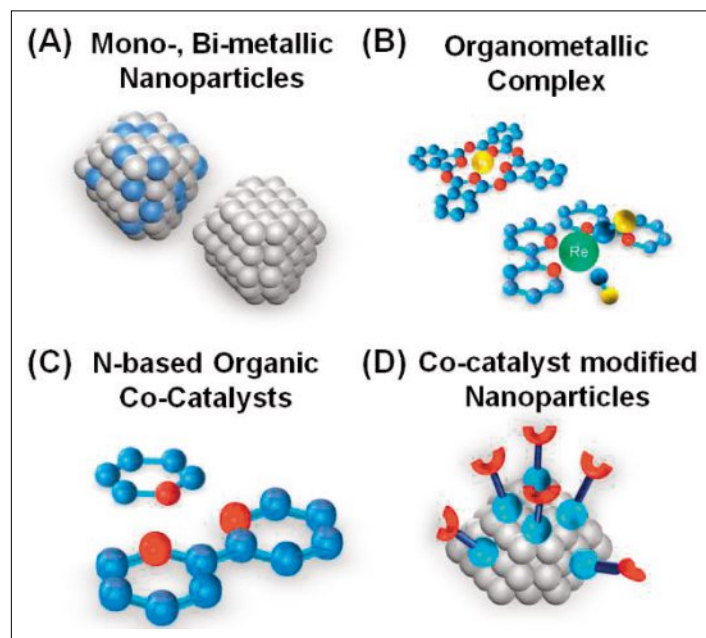

Fig. 4. Schematic representation of different types of (co-)catalysts for CO_2 electroreduction. Red spheres represent nitrogen atoms.

formate and Zn for CO production). Furthermore, other concepts like (i) increasing the surface area of the catalyst (*e.g.* metal foams), (ii) use of bimetallic catalysts, and (iii) use of organo-metallic complexes or nitrogen-rich ligands as (co-)catalysts might become more important for the CO_2 electrolysis.

[1] S. J. Davis, K. Caldeira, H. D. Matthews, *Science* **2010**, *329*, 1330.
[2] N. S. Lewis, D. G. Nocera, *Proc. Nat. Acad. Sci.* **2006**, *103*, 15729.
[3] R. Angamuthu, P. Byers, M. Lutz, A. L. Spek, E. Bouwman, *Science* **2010**, *327*, 313.
[4] M. E. Boot-Handford, J. C. Abanades, E. J. Anthony, M. J. Blunt, S. Brandani, N. Mac Dowell, J. R. Fernández, M.-C. Ferrari, R. Gross, J. P. Hallett, *Ener. Environ. Sci.* **2014**, *7*, 130.
[5] R. Winkler-Goldstein, A. Rastetter, *Green* **2013**, *3*, 69.
[6] M. Jentsch, T. Trost, M. Sterner, *Energy Procedia* **2014**, *46*, 254.
[7] Y. Hori, 'Electrochemical CO_2 reduction on metal electrodes. Modern aspects of electrochemistry', Springer, **2008**, pp 89-189.
[8] J. Ivy, 'Summary of electrolytic hydrogen production: milestone completion report', National Renewable Energy Lab, Golden, CO, US, **2004**.
[9] K. Zeng, D. Zhang, *Prog. Ener. Comb. Sci.* **2010**, *36*, 307.
[10] K. E. Ayers, E. B. Anderson, C. Capuano, B. Carter, L. Dalton, G. Hanlon, J. Manco, M. Niedzwiecki, *ECS Trans.* **2010**, *33*, 3.
[11] S. Marini, P. Salvi, P. Nelli, R. Pesenti, M. Villa, M. Berrettoni, G. Zangari, Y. Kiros, *Electrochim. Acta* **2012**, *82*, 384.
[12] G. A. Olah, *Angew. Chem. Int. Ed.* **2005**, *44*, 2636.
[13] J. M. Ogden, *Annu. Rev. Ener. Environ.* **1999**, *24*, 227.
[14] 'IEA Energy Technology Essentials - Hydrogen Production & Distribution', *https://www.iea.org/publications/freepublications/publication/essentials5.pdf*, **2007**.
[15] R. Segers, *Biogeochemistry* **1998**, *41*, 23.
[16] G. Schmid, M. Fleischer, K. Wiesner, R. Krause, 'Electrochemical Reduction of CO_2', SCCER Annual Symposium **2014**, Paul Scherrer Institut, Switzerland.
[17] R. T. Warren, *Oil & Gas J.* **2012**, 110,
[18] Weekly Price Watch Report, *www.YnFx.com*, **2013**, pp 44.
[19] C. Higman, M. van der Burgt, 'Gasification', Gulf Professional Publishing, **2003**, ISBN 0-7506-7707-4.
[20] S. N. Bizzari, M. Blagoev, 'CEH Marketing Research Report: FORMIC ACID', **2010**.
[21] S. Moret, P. J. Dyson, G. Laurenczy, *Nature Commun.* **2014**, *5*, 4017.
[22] 'The Methanol Industry', *http://methanol.org/Methanol-Basics/The-Methanol-Industry.aspx*.
[23] A. Goeppert, M. Czaun, J.-P. Jones, G. S. Prakash, G. A. Olah, *Chem. Soc. Rev.* **2014**, *43*, 7995.
[24] 'Methanol Pricing', *http://emsh-ngtech.com/methanol/methanol-pricing/*.
[25] S. Ma, P. J. Kenis, *Curr. Op. Chem. Engin.* **2013**, *2*, 191.
[26] Y. Hori, H. Konishi, T. Futamura, A. Murata, O. Koga, H. Sakurai, K. Oguma, *Electrochim. Acta* **2005**, *50*, 5354.

[27] C. Delacourt, P. L. Ridgway, J. B. Kerr, J. Newman, *J. Electrochem. Soc.* **2008**, *155*, B42.
[28] D. T. Whipple, E. C. Finke, P. J. Kenis, *Electrochem. Solid-State Lett.* **2010**, *13*, B109.
[29] E. J. Dufek, T. E. Lister, M. E. McIlwain, *J. Appl. Electrochem.* **2011**, *41*, 623.
[30] A. Damjanovic, A. Dey, J. M. Bockris, *J. Electrochem. Soc.* **1966**, *113*, 739.
[31] Y. Hori, A. Murata, R. Takahashi, *J. Chem. Soc., Farad. Trans. 1* **1989**, *85*, 2309.
[32] Y. Chen, C. W. Li, M. W. Kanan, *J. Am. Chem. Soc.* **2012**, *134*, 19969.
[33] K. P. Kuhl, E. R. Cave, D. N. Abram, T. F. Jaramillo, *Ener. Environ. Sci.* **2012**, *5*, 7050.
[34] T. Hatsukade, K. P. Kuhl, E. R. Cave, D. N. Abram, T. F. Jaramillo, *PhysChemChemPhys* **2014**, *16*, 13814.
[35] P. J. Rheinländer, J. Herranz, J. Durst, H. A. Gasteiger, *J. Electrochem. Soc.* **2014**, *161*, F1.
[36] J. Durst, C. Simon, F. Hasché, H. A. Gasteiger, *J. Electrochem. Soc.* **2015**, *162*, F190.
[37] G. K. Wiberg, K. J. Mayrhofer, M. Arenz, *Fuel Cells* **2010**, *10*, 575.
[38] J. W. Wang, X. H. Liu, S. X. Mao, J. Y. Huang, *Nano Lett.* **2012**, *12*, 5897.
[39] Y. Lan, C. Gai, P. J. Kenis, J. Lu, *ChemElectroChem* **2014**, *1*, 1577.
[40] H. A. Gasteiger, S. S. Kocha, B. Sompalli, F. T. Wagner, *Appl. Catal. B: Environ.* **2005**, *56*, 9.
[41] K. E. Ayers, C. Capuano, E. B. Anderson, *ECS Trans.* **2012**, *41*, 15.
[42] J. Durst, A. Siebel, C. Simon, F. Hasche, J. Herranz, H. A. Gasteiger, *Ener. Environ. Sci.* **2014**, *7*, 2255.
[43] M. Carmo, D. L. Fritz, J. Mergel, D. Stolten, *Int. J. Hydrogen Ener.* **2013**, *38*, 4901.
[44] A. Filpi, M. Boccia, H. Gasteiger, *ECS Trans.* **2008**, *16*, 1835.
[45] J. R. Varcoe, R. C. Slade, *Fuel Cells* **2005**, *5*, 187.
[46] J. R. Varcoe, P. Atanassov, D. R. Dekel, A. M. Herring, M. A. Hickner, P. A. Kohl, A. R. Kucernak, W. E. Mustain, K. Nijmeijer, K. Scott, *Ener. Environ. Sci.* **2014**, *7*, 3135.
[47] J. Suntivich, K. J. May, H. A. Gasteiger, J. B. Goodenough, Y. Shao-Horn, *Science* **2011**, *334*, 1383.
[48] K. E. Ayers, E. B. Anderson, C. B. Capuano, M. Niedzwiecki, M. A. Hickner, C.-Y. Wang, Y. Leng, W. Zhao, *ECS Trans.* **2013**, *45*, 121.
[49] E. Fabbri, A. Habereder, K. Waltar, R. Kötz, T. Schmidt, *Catal. Sci. Technol.* **2014**, *4*, 3800.
[50] H. Yanagi, K. Fukuta, *ECS Trans.* **2008**, *16*, 257.
[51] C. C. Pavel, F. Cecconi, C. Emiliani, S. Santiccioli, A. Scaffidi, S. Catanorchi, M. Comotti, *Angew. Chem.* **2014**, *126*, 1402.
[52] K. Hara, A. Tsuneto, A. Kudo, T. Sakata, *J. Electrochem. Soc.* **1994**, *141*, 2097.
[53] C. Delacourt, J. Newman, *J. Electrochem. Soc.* **2010**, *157*, B1911.
[54] M. Ünlü, J. Zhou, P. A. Kohl, *J. Phys. Chem. C* **2009**, *113*, 11416.
[55] D. Seel, B. Benicewicz, L. Xiao, T. Schmidt, *Handbook of Fuel Cells* **2010**, vol. 5-6, John Wiley & Sons, Ltd.
[56] B. Xing, O. Savadogo, *Electrochem. Commun.* **2000**, *2*, 697.
[57] J. O. Jensen, D. Aili, M. K. Hansen, Q. Li, N. J. Bjerrum, E. Christensen, *ECS Trans.* **2014**, *64*, 1175.
[58] H.-R. Jhong, F. R. Brushett, L. Yin, D. M. Stevenson, P. J. A. Kenis, *J. Electrochem. Soc.* **2012**, *159*, B292.
[59] M. R. Thorson, K. I. Siil, P. J. Kenis, *J. Electrochem. Soc.* **2013**, *160*, F69.
[60] K. Wu, E. Birgersson, B. Kim, P. J. Kenis, I. A. Karimi, *J. Electrochem. Soc.* **2015**, *162*, F23.
[61] C. M. Zalitis, D. Kramer, A. R. Kucernak, *PhysChemChemPhys* **2013**, *15*, 4329.
[62] B. Kim, S. Ma, H.-R. M. Jhong, P. J. Kenis, *Electrochim. Acta* **2015**, *166*, 271.
[63] 'Aqueous carbonate electrolyte fuel cell', J. D. Giner, **1988**, Google Patents.

[64] E. Cairns, *Handbook of Fuel Cells* **2003**, John Wiley & Sons, Ltd., doi:10.1002/9780470974001.f104016.
[65] Y.-F. Hu, Z.-C. Liu, C.-M. Xu, X.-M. Zhang, *Chem. Soc. Rev.* **2011**, *40*, 3802.
[66] N. V. Rees, R. G. Compton, *Ener. Environ. Sci.* **2011**, *4*, 403.
[67] B. A. Rosen, A. Salehi-Khojin, M. R. Thorson, W. Zhu, D. T. Whipple, P. J. Kenis, R. I. Masel, *Science* **2011**, *334*, 643.
[68] J. L. DiMeglio, J. Rosenthal, *J. Am. Chem. Soc.* **2013**, *135*, 8798.
[69] J. Medina-Ramos, J. L. DiMeglio, J. Rosenthal, *J. Am. Chem. Soc.* **2014**, *136*, 8361.
[70] Q. Lu, J. Rosen, F. Jiao, *ChemCatChem* **2015**, *7*, 38.
[71] X. Lu, D. Y. Leung, H. Wang, M. K. Leung, J. Xuan, *ChemElectroChem* **2014**, *1*, 836.
[72] M. Mahmood, D. Masheder, C. Harty, *J. Appl. Electrochem.* **1987**, *17*, 1159.
[73] M. Alvarez-Guerra, S. Quintanilla, A. Irabien, *Chem. Engin. J.* **2012**, *207*, 278.
[74] J. Wu, F. G. Risalvato, F.-S. Ke, P. Pellechia, X.-D. Zhou, *J. Electrochem. Soc.* **2012**, *159*, F353.
[75] M. Alvarez-Guerra, A. Del Castillo, A. Irabien, *Chem. Engin. Res. Design* **2014**, *92*, 692.
[76] A. Del Castillo, M. Alvarez-Guerra, A. Irabien, *AIChE J.* **2014**, *60*, 3557.
[77] S. Zhang, P. Kang, T. J. Meyer, *J. Am. Chem. Soc.* **2014**, *136*, 1734.
[78] B. Podlovchenko, E. Kolyadko, S. Lu, *J. Electroanal. Chem.* **1994**, *373*, 185.
[79] X. Min, M. W. Kanan, *J. Am. Chem. Soc.* **2015**, *137*, 4701.
[80] S. Lee, J. D. Ocon, Y.-i. Son, J. Lee, *J. Phys. Chem. C* **2015**, *119*, 4884.
[81] N. Furuya, S. Koide, *Electrochim. Acta* **1991**, *36*, 1309.
[82] Y. Chen, M. W. Kanan, *J. Am. Chem. Soc.* **2012**, *134*, 1986.
[83] N. Furuya, T. Yamazaki, M. Shibata, *J. Electroanal. Chem.* **1997**, *431*, 39.
[84] F. Köleli, T. Atilan, N. Palamut, A. Gizir, R. Aydin, C. Hamann, *J. Appl. Electrochem.* **2003**, *33*, 447.
[85] B. Innocent, D. Liaigre, D. Pasquier, F. Ropital, J.-M. Léger, K. Kokoh, *J. Appl. Electrochem.* **2009**, *39*, 227.
[86] J. Wu, F. G. Risalvato, P. P. Sharma, P. J. Pellechia, F.-S. Ke, X.-D. Zhou, *J. Electrochem. Soc.* **2013**, *160*, F953.
[87] R. Parajuli, J. B. Gerken, K. Keyshar, I. Sullivan, N. Sivasankar, K. Teamey, S. S. Stahl, E. B. Cole, *Topics in Catal.* **2015**, *58*, 57.
[88] M. Mahmood, D. Masheder, C. Harty, *J. Appl. Electrochem.* **1987**, *17*, 1223.
[89] C. E. Tornow, M. R. Thorson, S. Ma, A. A. Gewirth, P. J. Kenis, *J. Am. Chem. Soc.* **2012**, *134*, 19520.
[90] H. R. Jhong, F. R. Brushett, P. J. Kenis, *Adv. Ener. Mater.* **2013**, *3*, 589.
[91] S. Ma, Y. Lan, G. M. Perez, S. Moniri, P. J. Kenis, *ChemSusChem* **2014**, *7*, 866.
[92] O. A. Baturina, Q. Lu, M. A. Padilla, L. Xin, W. Li, A. Serov, K. Artyushkova, P. Atanassov, F. Xu, A. Epshteyn, T. Brintlinger, M. Schuette, G. E. Collins, *ACS Catalysis* **2014**, *4*, 3682.
[93] W. Zhu, R. Michalsky, O. n. Metin, H. Lv, S. Guo, C. J. Wright, X. Sun, A. A. Peterson, S. Sun, *J. Am. Chem. Soc.* **2013**, *135*, 16833.
[94] D. Kim, J. Resasco, Y. Yu, A. M. Asiri, P. Yang, *Nature Commun.* **2014**, *5*, 4948.
[95] C. Costentin, M. Robert, J.-M. Savéant, *Chem. Soc. Rev.* **2013**, *42*, 2423.
[96] J. Qiao, Y. Liu, F. Hong, J. Zhang, *Chem. Soc. Rev.* **2014**, *43*, 631.
[97] M. Fujihira, Y. Hirata, K. Suga, *J. Electroanal. Chem. Interfacial Electrochem.* **1990**, *292*, 199.
[98] G. B. Balazs, F. C. Anson, *J. Electroanal. Chem.* **1992**, *322*, 325.
[99] J. D. Froehlich, C. P. Kubiak, *Inorg. Chem.* **2012**, *51*, 3932.